Entrainment in Annular Two-Phase Flow under Steady and Transient Flow Conditions

H. LANGNER and F. MAYINGER
Institut für Verfahrenstechnik
Technische Universität Hannover, West Germany

ABSTRACT

In the theoretical part, a system of differential equations is formulated and solved numerically to calculate the net-entrainment mass-flow rate in the gas core of annular two-phase flow. In the conservation laws of mass, momentum and energy - which form the base of the above mentioned system of equations - a semi-empirical model established by Levy is used to calculate the interfacial shear stress between the vapour phase and the liquid film at the tube wall.

In order to test the theory, experiments in an externally heated tube have been performed with the model-fluid R 12. The entrainment mass-flow rate was measured by the aid of an optical method, which delivered very good information about the structure of annular flow. The experimental results are compared with the theoretical prediction. The agreement is quite satisfactory.

NOMENCLATURE

Symbol	Quantity	SI-Unit
D	diameter	m
D_h	hydraulic diameter	m
F	cross-section area	m^2
$\dot{M}$	mass flow rate	kg/s
r	radius	m
s_F	film thickness	m; mm
g_n	acceleration of gravity	9.8 m/s^2
r_V	specific latent heat of vaporization	kJ/kg
z	characteristic length	m
$\dot{m}$	mass flux density	$kg/m^2 s$
p	pressure	bar; N/m^2
$\dot{q}$	heat flux density	W/m^2 ; W/cm^2

u; v; w	velocity	m/s
ϱ	mass density	kg/m³
τ_i	interfacial shear stress	N/m²
$x = \dot{M}_{Fl}/\dot{M}_{ges}$	quality	-
$\Delta p/\Delta z$	pressure drop per unit length	N/m²m
E	dimensionless entrainment numbers	-
ε	void fraction	-

Indices

Ent	Entrainment
ges	total
D	related to the vapour phase
Fl	related to the liquid phase
core; c	related to the gas-core of an annular flow
DO	Dryout

INTRODUCTION

In lack of detailed information about the exact phase distribution in the annular flow regime, many theoretical models base on the assumption that the liquid phase flows as a thin film with a smooth surface at the tube wall, while the vapour phase - due to its lower density - with higher velocity in the center of the channel.

These models failed to describe certain phenomena, so for example pressure drop or film thickness, as they occur in a real annular flow. The comparison between measured and calculated results show that the deviation is sometimes in the range of 100 percent.

More realistic is the conception that a part of the liquid phase is carried away in form of droplets by the vapour phase in the gas core of the annular flow.

The knowledge of the real phase distribution - in vapour, liquid film at the tube wall, and entrainment - especially in diabatic two-phase flow becomes more and more important in the last years, since the heat-flux densities in heat exchangers increase. Especially in the core of a nuclear boiling-water reactor with high void fraction the liquid fraction entrained is important for calculating critical heat flux, pressure drop from a momentum balance or for describing the heat transfer as well in the pre-dryout or in the post-dryout region for steady state and for transient (blowdown) conditions in the case of a LOCA (loss-of-coolant accident).

For the theoretical prediction of the entrainment mass flow rate a system of differential equations is used including the conservation laws for mass, energy and momentum and a semi-empirical model evaluated by Levy to estimate the interfacial shear stress between the phases.

THEORY

Assumptions and Definitions

We assume that

- the flow is one-dimensional
- all entrained liquid has a common velocity $w_{ENT}(z,t)$ which is different from the gas-phase velocity $w_D(z,t)$
- the gas core radius r_1 is constant over z and in time
- there is no evaporation or condensation on entrained droplets

and define E as the ratio of entrainment mass flow to total liquid mass flow in the duct at position z at time t

$$E = E(z;t) = \frac{\dot{M}_{Ent}}{\dot{M}_{Fl,ges}} = \frac{\dot{M}_{Ent}}{\dot{M}_{ges}(1-x)} \tag{1}$$

By differentiating eq. (1) with respect to the channel length z, one obtains an equation that allows the calculation of the gradient $d\dot{M}_{ENT}/dz$.t.m. the change of the entrainment mass flow rate with respect to the channel length, provided E (z,t) is known:

$$\frac{\partial \dot{M}_{Ent}}{\partial z} = \dot{M}_{ges}(1-x)\left[\frac{\partial E}{\partial z} + E\left[\frac{1}{\dot{M}_{ges}}\frac{\partial \dot{M}_{ges}}{\partial z} - \frac{1}{(1-x)}\frac{\partial x}{\partial z}\right]\right] \tag{2}$$

For steady-state conditions eq. (2) reduces to eq. (3), because the total mass flow rate is not a function of the channel length.

$$\left.\frac{d\dot{M}_{Ent}}{dz}\right|_{stat} = \dot{M}_{ges}\cdot\left[(1-x)\frac{dE}{dz} - E\cdot\frac{dx}{dz}\right] \tag{3}$$

In addition to eq. (3) one must formulate the momentum balance over the cross section of the gas core of the annular flow to calculate the gradient dE/dz, and the energy balance over the heated length of the channel to calculate the gradient dx/dz.

Momentum and energy balance

The basic conservation principle for momentum can be stated as

[The rate of change of momentum] = [Momentum outflow rate] − [Momentum inflow rate] + [Momentum storage rate] = [The sum of the forces acting on the control volume]

Fig. 1 shows the forces acting on the control volume. The radial boundary of this control volume is the liquid film surface, because the important physical phenomena for the droplet entrainment occur

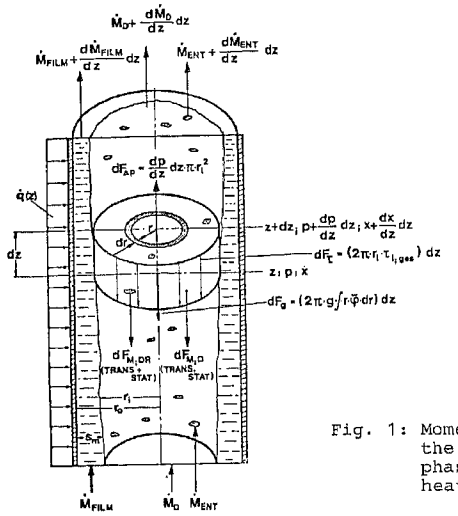

Fig. 1: Momentum balance across the gas core of a two-phase annular flow with heat addition

at this surface.

In accordance to fig. 1 the single forces are

a driving force resulting from the pressure drop
an interfacial shear stress force
a gravitation force and
a momentum force resulting from the phases in the gas core.

The momentum balance can be written as

$$\frac{\partial}{\partial z}(\dot{m}_D w_D + \dot{m}_{ENT} w_{ENT})\cdot dz \cdot \int_0^{r_i} 2\pi r\,dr + \frac{\partial}{\partial t}(\dot{m}_D + \dot{m}_{ENT})\,dz \cdot \int_0^{r_i} 2\pi r\,dr = \tag{4}$$

$$\pi r_i^2 \left(p - \left(p + \frac{\partial p}{\partial z}dz\right)\right) - 2\pi r_i \cdot \tau_i \cdot dz - \int_0^{r_i} 2\pi r\,dr \cdot \bar{\varrho} \cdot g_n \cdot dz$$

These simplifications are already explained in the chapter "Assumptions and Definitions".

By introducing E as defined in eq. (1), we have

$$\pi r_o^2 \cdot \frac{\partial}{\partial z}\left(\dot{m}_{ges}^2 \cdot \left(\frac{r_o}{r_i}\right)^2 \cdot \left[\frac{X}{\varrho_D} + \frac{E(1-x)}{\varrho_{FI}}\right]\Big[X + E(1-x)\Big]\right)dz + \ldots \tag{5}$$

$$\ldots + \pi r_i^2 \left(\dot{m}_{ges}(1-E)\frac{\partial x}{\partial t} + \dot{m}_{ges}(1-x)\frac{\partial E}{\partial t} + \big(X + E(1-x)\big)\frac{\partial \dot{m}_{ges}}{\partial t}\right)dz =$$

$$\pi r_i^2 \left(p - \left(p + \frac{\partial p}{\partial z}dz\right)\right) - 2\pi r_i \cdot \tau_i \cdot dz - \int_0^{r_i} 2\pi r \cdot g \cdot \big(\varrho_D \cdot \varepsilon + \varrho_{FI} \cdot (1-\varepsilon)\big)\,dr \cdot dz$$

From this momentum equation one can calculate $\partial E/\partial z$, provided τ_i and $\partial p/\partial z$ are known. For steady state conditions, one can set the

time-depending gradients in eq. (5) equal to zero, which leads to eq. (6), which can be used to calculate the gradient dE/dz in a steady state two-phase flow with heat addition.

$$\frac{dE}{dz} = -\left[\frac{2\cdot\tau_i - \frac{dp}{dz} + \frac{x+E(1-x)}{x+E(1-x)\varrho_D/\varrho_{FI}}\cdot g\cdot\varrho_D}{\dot{m}_{ges}^2\left(\frac{r_o}{r_i}\right)^4\left[\big(x+E(1-x)\big)\cdot\left(\frac{1-x}{\varrho_D}\right)+\left(\frac{x}{\varrho_D}-\frac{E(1-x)}{\varrho_{FI}}\right)\cdot(1-x)\right]} + \frac{dx}{dz}\cdot\frac{\tau_i}{\tau_2}\right] = f\left(E; x; \tau_i; \frac{dp}{dz}; \frac{\varrho_D}{\varrho_{FI}}; \dot{m}_g; r_o\right) \tag{6}$$

where

$$\tau_1 = \big(x+E(1-x)\big)\left(\frac{1}{\varrho_D} - \frac{E}{\varrho_{FI}}\right) + \left(\frac{x}{\varrho_D} + \frac{E(1-x)}{\varrho_{FI}}\right)\cdot(1-E)$$

$$\tau_2 = \big(x+E(1-x)\big)\left(\frac{1-x}{\varrho_{FI}}\right) + \left(\frac{x}{\varrho_D} + \frac{E(1-x)}{\varrho_{FI}}\right)\cdot(1-x)$$

Eq. (6) includes the simplification that for relative thin films the ratio of inner tube radius to radius of the film surface is very close to 1 and the ratio does not change very much along the channel, so that the gradient d $(ro/ri)^2$ /dz was set equal to zero.

Furthermore it is interesting to see which effect is the most essential one for the occurance of liquid entrainment in annular flow. Fig. 2 gives an idea of the influence of the single terms that have been discussed in the entrainment equation. (eq. 6)

The dominating effect is the pressure drop, followed by the interfacial shear stress term.

In addition to the momentum balance an energy balance over the heated length of the channel is required to calculate the change of the quality with respect to the channel length. Further-

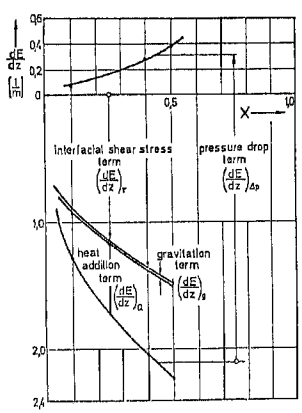

Fig. 2: Single Terms Influencing the Entrainment Rate

more the Levy model to determine the interfacial shear stress /5/ is required. If the pressure drop of the two-phase flow is known from measurements or from the calculation with one of the well-known computer codes - for example Relap 4 - the set of differential equations can be solved numerically by the aid of a difference method of the Runge-Kutta type.

TEST RESULTS

Measuring technique

To test the theory measurements of the liquid fraction entrained had been carried out, using an optical measuring technique similar to an arrangement introduced by Hewitt and Arnold /1/ in 1964.

As shown in fig. 3 a slit device to separate the liquid film and the droplet-loaded vapour core, with a glass tube to expose the flow and a glass window to get an axial view in flow direction, was positioned at the end of an electrically heated tube. We used a stainless steel tube with an inner diameter of 0.014 m and a heated length of 5 m.

The advantage of this so-called "axial-view-method" is demonstrated in fig. 4. The photo on the right hand side delivers much more information than the photo taken in the same moment rectangular to the flow direction.

With a special evaluation-method - described in detail in /2/ and /3/ - the entrainment mass-flow rate could be analyzed from high speed movies or from a series of single photos.

Steady state tests

In a first step tests at steady state conditions had been carried out using the model fluid R 12. The entrainment mass flow had been measured in dependance of the following parameters.

total mass flow rate	$\dot{M}_{ges}$	= 300 ... 1000 kg/m²s
local quality	x_{ges}	= 0.2 ... 0.94
system pressure	P_{ges}	= 8 ... 14 bar

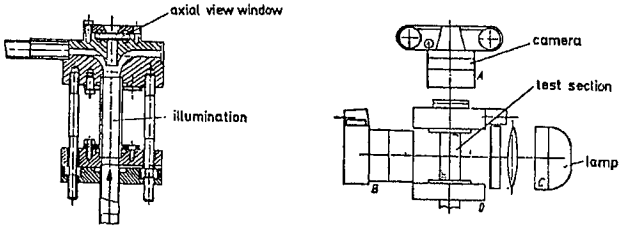

Fig. 3: Slit device and camera arrangement

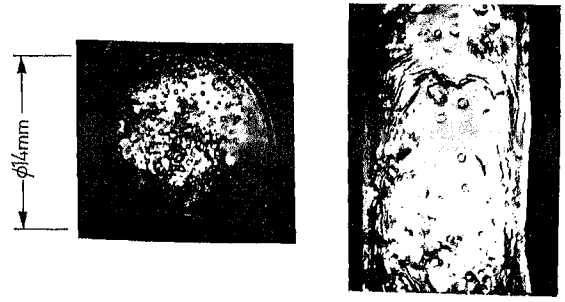

Fig. 4: Comparison of the measuring techniques

test section length	z	total heated length 5 m
inlet subcooling	Δh_{in}	= 3 ... 20 kJ/kg

The experimental results show that the total mass flow rate and the local quality are the most important parameters influencing the droplet entrainment, while the other parameters - listed above - did not affect the entrainment mass flow rate essentially, as demonstrated in fig. 5 and fig. 6.

The experimental results show good quantitative and qualitative agreement with measurements in the literature /4/.

For the recalculation of the test results the measurements, shown in fig. 5, are represented in form of the dimensionless en-

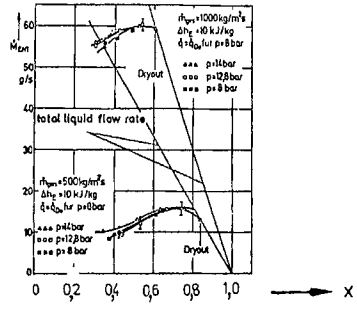

Fig. 5: Entrainment mass flow rate as a function of quality, for different total mass flow rates $\dot{m}_{ges}$ and system pressures p

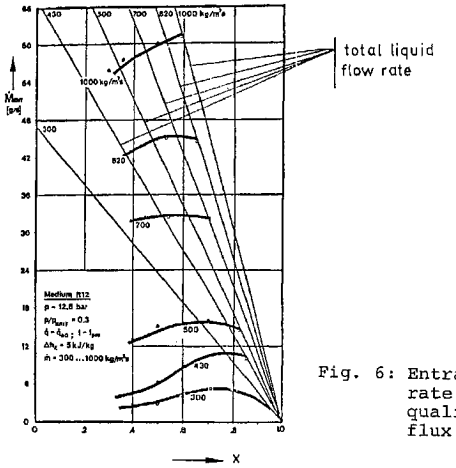

Fig. 6: Entrainment mass flow rate as a function of quality and total mass flux density

trainment number E as defined in eq. (1) - see fig. 7.

Fig. 8a and b show the recalculation of characteristic test results with the theory. The agreement between experiments and theory is quite satisfactory.

The maximum deviation (of about 15 percent) occurs especially in the region of low qualities with thick and wavy films where the phase distribution is not fully established. To verify the theory for other media than R 12, entrainment measurements with water-steam two-phase flow carried out by Keeys /4/ had been recalculated, too, see Fig. 9.

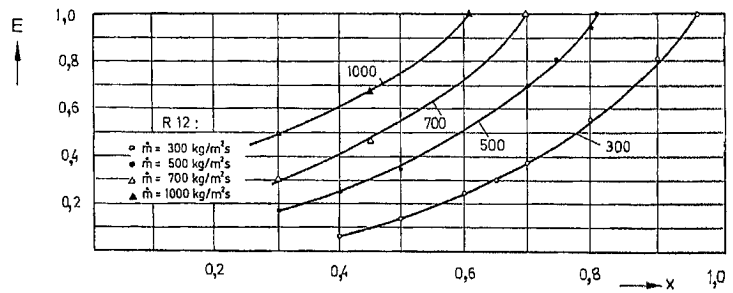

Fig. 7: Steady-state entrainment measurements with R 12

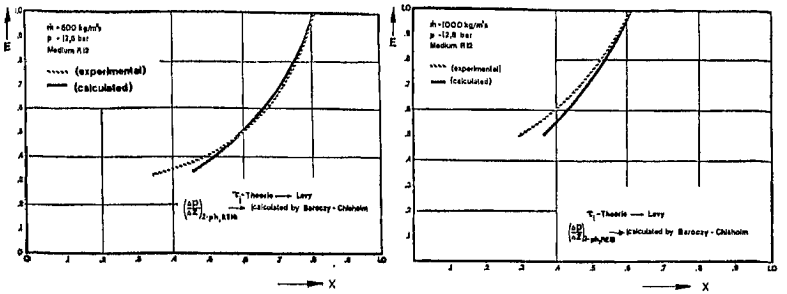

Fig. 8: Comparison between measurements and theory for R 12 flow

These authors measured the entrainment mass flow rate at a system pressure of 70 bars and at relatively high mass fluxes. The comparison between measured and calculated data for these tests show good agreement, too.

Transient Tests

In addition to the steady state tests, the liquid fraction entrained was measured in a transient annular flow corresponding to depressurization conditions in a nuclear reactor core during blowdown.

The entrainment mass flow measurement had been carried out in the annular flow regime immediately before dryout, see fig. 10, and the results of these measurements are shown in fig. 11. With larger acceleration of the phases - corresponding to larger cross section areas of the simulated break - the amount of droplets entrained from the liquid film surface increases rapidly, too.

At relatively low acceleration of the phases a "quasi-stationary" entrainment behaviour has been observed, that means decrea-

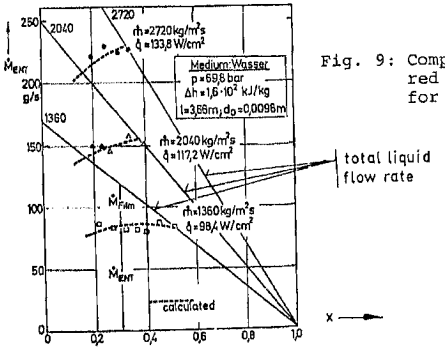

Fig. 9: Comparison between measured and calculated data for water-steam flow /4/

sing entrainment mass flow at high void fraction combined with very thin liquid films at the tube wall /6/. At high acceleration rates the interfacial shear stress forces are so high that liquid droplets are torn away even from very thin films, so that the entrainment mass flow increases until the dryout occurs. Due to the rise of the liquid fraction entrained the reduction of film thickness is very significant, so that there is a very short annular flow period at great break areas - see fig. 10.

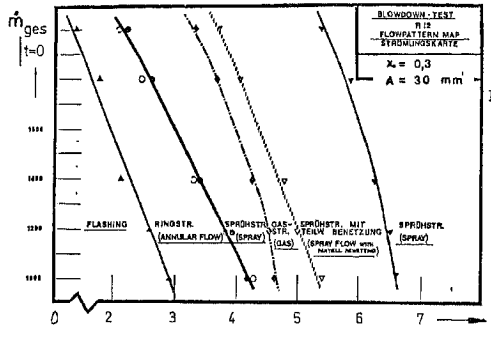

Fig. 10: Transient flow pattern map

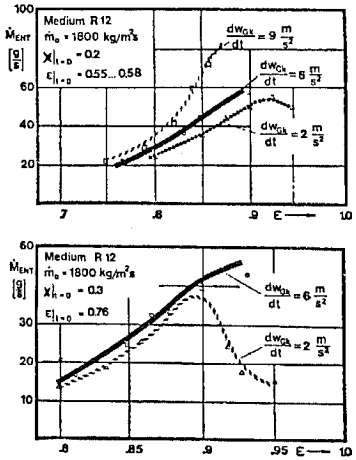

LOCA-conditions

$\frac{dw}{dt} = 9 \frac{m}{s} \Longrightarrow$ "1,4-F" break

$\frac{dw}{dt} = 6 \frac{m}{s} \Longrightarrow$ "1-F" break

$\frac{dw}{dt} = 2 \frac{m}{s} \Longrightarrow$ "0,2-F" break

Fig. 11: Transient entrainment mass flow rate

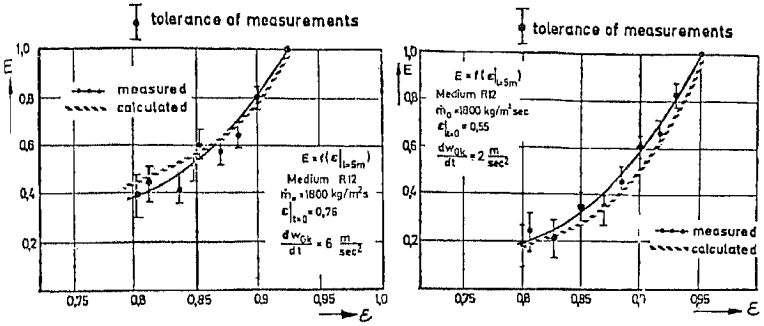

Fig. 12: Comparison between measured and calculated transient entrainment data

Fig. 12 shows the transient entrainment data in form of E as a function of the void fraction and their recalculation with the presented theory. The pressure drop must be taken from transient measurements to solve the set of equations assuming that the interfacial shear stress model of Levy is valid for transient conditions.

As the measurements of the pressure drop under transient conditions are very difficult and incorrect, the agreement between the theoretical forecast and the measurements is not very good.

By correcting the transient pressure drop measurements with the empirical factor C* = 0,7 the deviation between measured and calculated entrainment data is in the range of 20 percent as shown in fig. 12.

SUMMARY

A set of differential equations basing on the conservation laws for mass, energy and momentum leads to the description of the entrainment mass flow in the annular flow regime as well for steady state as for transient conditions. For the verification of this theory measurements with the model fluid R 12 had been carried out using an optical measuring technique. The comparison between measured and calculated entrainment data shows satisfactory agreement.

LITERATURE

1. Arnold, C.R., and Hewitt, G.F. 1967. Further Developments in the Photography of Two-Phase Gas-Liquid Flow. Journ. of Photographic Sci. 15: 97.

2. Mayinger, F., and Langner, H. 1976. Steady State and Transient Entrainment Behaviour in Upwards Co-Current Annular Flow. Proceedings of the "NATO-Advanced Study Institute on Two-Phase Flow and Heat Transfer". Istanbul (Turkey).

3. Langner, H., and Mayinger, F. 1977. Der Einsatz einer optischen Meßtechnik zur Bestimmung des Entrainmentverhaltens einer Zweiphasenströmung unter stationären und instationären Blowdown-Bedingungen. Paper presented at the 2nd KTG-Fachtagung, Hanover.

4. Keeys, R.K., and Ralph, R. 1970. The Effect of Heat Flux on Liquid Entrainment in Annular Two-Phase Flow in a Vertical Tube. AERE-Report No. 6294.

5. Levy, S. 1966. Prediction of Annular Two-Phase Flow with Liquid Entrainment. Int. Jour. of Heat & Mass Transfer 9: 171.

6. Hewitt, G.F. 1970. Hall-Taylor. Annular Two-Phase Flow. Pergamon Press, Oxford.